ISSN 1070-3284, Russian Journal of Coordination Chemistry, 2024, Vol. 50, No. 2, pp. 145–155. © Pleiades Publishing, Ltd., 2024.

# Lanthanide Complexes of Related Click Tripodal 1,2,3-Triazole-Containing Ligands on the $Ph_3P(O)$ Platform. The $N^2$ and $N^3$ Coordination of Triazole Fragments

**A. G. Matveeva[a], *, M. P. Pasechnik[a], R. R. Aysin[a], O. V. Bykhovskaya[a], S. V. Matveev[a], T. V. Baulina[a], I. Yu. Kudryavtsev[a], A. N. Turanov[b], V. K. Karandashev[c, d], and V. K. Brel[a]**

[a] *Nesmeyanov Institute of Organoelement Compounds, Russian Academy of Sciences, Moscow, Russia*

[b] *Institute of Solid State Physics, Russian Academy of Sciences, Chernogolovka, Moscow oblast, Russia*

[c] *Institute of Microelectronics Technology and High Purity Materials, Russian Academy of Sciences, Chernogolovka, Moscow oblast, Russia*

[d] *National University of Science and Technology (MISiS), Moscow, Russia*

**e-mail: matveeva@ineos.ac.ru*

Received May 16, 2023; revised July 5, 2023; accepted July 6, 2023

**Abstract**—The coordination and extraction properties of two related tripodal ligands differed by types of addition of the triazole fragment and linker length in the {2-[(4-Ph-1,2,3-triazol-1-yl)$CH_2CH_2O$]$C_6H_4$}$_3$P(O) ($L^1$) and {2-[(1-Ph-1,2,3-triazol-4-yl)$CH_2O$]$C_6H_4$}$_3$P(O) ($L^2$) are compared. The structures of the complexes [$La(NO_3)_3L^1$] (**I**) and [$Lu(NO_3)_3L^1$] (**II**) are studied in the solid phase (elemental analysis, IR and Raman spectroscopy) and in solutions (IR and multinuclear $^1H$, $^{13}C$, and $^{31}P$ NMR spectroscopy). A normal coordinate analysis at the TPSS-D4/Def2-SVP level is performed for an isolated molecule of the model complex [La{P(*O*),$N^3$,$N^2$-$L^3$}(O,O-$NO_3$)$_3$] ($L^3$ = {2-[(4-Me-1,2,3-triazol-1-yl)$CH_2CH_2O$]$C_6H_4$}$_3$-P(O)). According to the set of spectral and quantum chemical data, ligand $L^1$ exhibits the tridentate P(O),$N^2$,$N^2$ coordination in lanthanide complexes **I** and **II**. These are neutral complexes in the solid state and in $CD_3CN$ solutions, and the dynamic equilibrium of the neutral and ionic complexes is observed in $CDCl_3$. Unlike ligand $L^1$, ligand $L^2$ exhibits the tetradentate P(O),$N^3$,$N^3$,$N^3$ coordination in the [$Ln(NO_3)_3L^2$] complexes with the same metals (Ln = $La^{3+}$, $Lu^{3+}$) in solutions. The efficiency of extraction of microquantities of *f* elements from the aqueous phase to 1,2-dichloroethane by compounds $L^1$ and $L^2$ is discussed in comparison with the structures of the complexes of both ligands in solutions.

**Keywords:** lanthanide complexes, tripodal triazole-containing ligands, vibrational spectroscopy, NMR spectroscopy, structure in solid state, structure in solutions, extraction

**DOI:** 10.1134/S1070328423601000

## INTRODUCTION

Increasing number of examples of tripodal ligands containing 1,2,3-triazole cycles in the pendants appears due to a wide use of the Cu(I)-catalyzed azide–alkyne cycloaddition (first example of the so-called "click" reaction) [1–8]. The complexes of these ligands with metals have a series of promising practical applications. The complexes with Fe(II) and Co(II) demonstrate the properties of spin crossovers [1, 8], and the complexes with lanthanides and transition metals are of interest for magnetic resonance imaging, catalysis [1, 2, 5, 7], development of photo- and electroluminescent materials [1, 2, 4], and medical biological purposes [3].

When studying the complex formation of the related 1,2,3-triazole-containing ligands, the strength and physicochemical properties of the complexes (catalytic, photophysical, magnetic, and other) were found to depend substantially on the N-coordination mode of the 1,4-substituted triazole fragment [2, 9–13]. The 1,4-substituted 1,2,3-triazole fragment is known to be capable of interacting with the metal cations via the $N^3$ or $N^2$ atoms [1, 2, 4–6]. The 1,2,3-triazole fragment is most frequently bound to the metal cation via the $N^3$ atom with the formation of stronger complexes, which is explained by a higher electron density on this atom [2]. The $N^2$ coordination is observed rather rarely: usually when the coordination to the $N^3$ atom is inaccessible or hindered [1, 2, 6]. An additional stronger donor center also favors the $N^2$ coordination of the triazole fragment in the chelate metallocycle. In the majority of the described complexes of 1,2,3-triazole-containing ligands, the N-coordination mode of the single chelate metallocycle can easily be identified.

In this work, we used vibrational and NMR spectroscopy and quantum-chemical calculations to analyze how the 1,2,3-triazole fragment of the related tripodal ligands (tris{2-[2'-(4"-phenyl-1",2",3"-triazol-1"-yl)ethoxy]phenyl}phosphine oxide ($L^1$), tris{2-[(1"-phenyl-1",2",3"-triazol-4"-yl)methoxy]phenyl}phosphine oxide ($L^2$), tris{2-[2'-(4"-methyl-1",2",3"-triazol-1"-yl)ethoxy]phenyl}phosphine oxide ($L^3$) (Scheme 1)) is involved in coordination with lanthanides in a more complicated structural context where other triazole fragments and the P(O) group of the platform compete for binding with the metal. For this purpose, we compared the coordination and extraction properties of two closely related ligands $L^1$ [14] and $L^2$ [15] differed by the type of addition of the triazole fragment and the linker length.

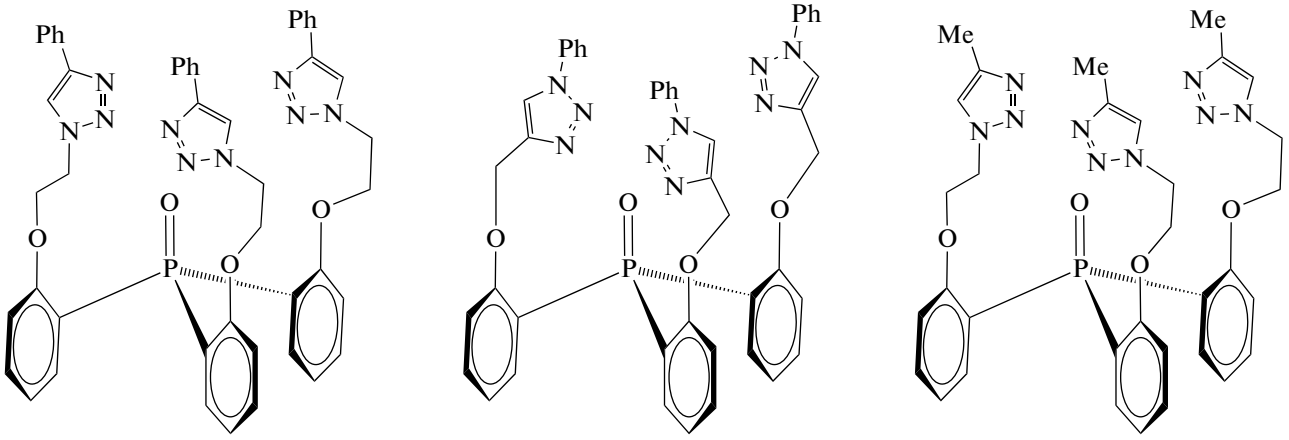

$L^1$ $L^2$ $L^3$

**Scheme 1.**

The extraction properties were studied for the extraction of microquantities of U(VI), Th(IV), and Eu(III) from aqueous solutions to 1,2-dichloroethane, and the coordination properties were studied for complex formation with La(III) and Lu(III) nitrates. The metals were chosen for several reasons. First, the coordination sphere of polytopic tripodal ligands is favorable for the formation of complexes with bulky multicharge lanthanide cations having high coordination numbers [16]. Second, lanthanides form complexes with both O- and N-donor ligands [17–19]. Third, the lanthanide complexes have numerous promising practical applications [1, 3, 4, 17–19], and the nonparamagnetic representatives of the series (La and Lu) make it possible to successfully use NMR spectroscopy to study the structures of the complexes in solutions.

The complexes $[La(L^1)(NO_3)_3]$ (**I**) and $[Lu(L^1)(NO_3)_3]$ (**II**) synthesized in this work were characterized by elemental analysis and IR and Raman spectroscopy. The $[Pd(L^1)Cl_2]$ (**III**) [14] and $[UO_2(L^1)(NO_3)_2]$ [20] complexes are also known. For the correct interpretation of the vibrational spectra, we performed the quantum chemical calculations of the geometry and normal vibrational frequencies and shapes of the model complex $[La(L^3)(NO_3)_3]$ (**IV**). Ligand $L^3$ with Me substituents in the triazole cycle (Scheme 1) was used as a simpler model in the quantum-chemical calculations instead of ligand $L^1$. The structures of complexes **I** and **II** in solutions ($CD_3CN$ and $CDCl_3$) were studied by IR and multinuclear ($^1H$, $^{13}C$, $^{31}P$) NMR spectroscopy. Complexes $[La(L^2)(NO_3)_3]$ (**V**) and $[Lu(L^2)(NO_3)_3]$ (**VI**) were synthesized and studied earlier [15]. The data on the structures of the lanthanide complexes of ligands $L^1$ and $L^2$ in solutions were compared with the efficiency of *f* element extraction by compounds $L^1$ and $L^2$.

## EXPERIMENTAL

Organic solvents (reagent grade) were dehydrated and purified using standard procedures [21]. Deuterated solvents $CD_3CN$ and $CDCl_3$ (Acros) were used as received.

IR spectra were recorded on a Bruker Tensor 37 FT-IR spectrometer for solid samples (as KBr pellets) in the range of 4000–400 $cm^{-1}$; and in the range of 4000–950 $cm^{-1}$ for 0.01 M solutions in $CDCl_3$ ($CaF_2$ cuvette path length 0.23 mm) and for 0.02 M solutions in $CD_3CN$ ($CaF_2$ cuvette path length 0.06 mm).

Raman spectra in the range of 3500–100 $cm^{-1}$ were detected on a Jobin-Yvon LabRAM 300 spectrometer equipped with a microscope and a laser CCD detector. The line of a He–Ne laser with a wavelength of

632.8 nm and the power at most 2 mW was used as the exciting line.

The $^{1}H$, $^{13}C\{^{1}H\}$, and $^{31}P\{^{1}H\}$ NMR spectra of solutions of the synthesized compounds in $CDCl_3$ (0.01 M) and $CD_3CN$ (0.01 M) were recorded on a Bruker Avance 500 instrument ($^{1}H$, $^{13}C$, and $^{31}P$ working frequencies were 500.13, 125.77, and 242.97 MHz, respectively). The signals of residual protons and carbon atoms of the solvent in the $^{1}H$ and $^{13}C$ NMR spectra were used as internal references, and the determination accuracy of chemical shifts was at least 0.01 and 0.03 ppm, respectively. The chemical shifts in the $^{31}P$ NMR spectra were presented relative to 85% $H_3PO_4$ as the external standard.

Melting points were measured with shortened Anschutz thermometers in a special block using capillary tubes.

The contents of C, H, and N were determined on a Carlo Erba 1106 instrument.

Salts $La(NO_3)_3{\cdot}6H_2O$ (reagent grade) and $Lu(NO_3)_3{\cdot}xH_2O$ (Aldrich) were used as received. The water content ($x = 3$) in the commercial preparation of lutetium nitrate was determined experimentally. Salts $UO_2(NO_3)_2{\cdot}6H_2O$ (reagent grade), $Th(NO_3)_4{\cdot}5H_2O$ (pure grade), and $Eu(NO_3)_3{\cdot}6H_2O$ (pure grade) were used without additional purification.

Ligands $L^1$ [14] and $L^2$ [15] were synthesized using the known procedures.

**General procedure for the synthesis of the complexes.** Complexes **I** and **II** were synthesized at a reagent ratio of 1 : 1. A solution of the salt was added dropwise with stirring to a solution of ligand $L^1$. The transparent solution was stirred at 45–50°C for 3 h and stored at room temperature for ~12 h. The solvent was evaporated, ether was added, and the precipitate was separated and dried in vacuo. The residue was dried in vacuo (1–2 mmHg) over $P_2O_5$ at 62°C for 3 h. Unfortunately, we failed to grow crystals suitable for XRD.

The data on the IR, Raman, and multinuclear NMR spectra of the synthesized compounds and the scheme with the numeration of the ligand atoms are given in the Supplementary Information (Scheme S1, Figs. S1–S21).

**Complex $[La(L^1)(NO_3)_3]$ (I).** A solution of $La(NO_3)_3{\cdot}6H_2O$ (0.0393 g, 0.0907 mmol) in MeCN was added to a solution of ligand $L^1$ (0.0761 g, 0.0907 mmol) in MeCN. The yield was 0.0900 g (85%), $T_m > 185$°C (decomp.).

For $C_{48}H_{42}N_{12}O_{13}PLa$

| | | | |
|---|---|---|---|
| Anal. calcd., % | C, 49.48 | H, 3.61 | N, 14.43 |
| Found, % | C, 49.34 | H, 3.63 | N, 14.41 |

**Complex $[Lu(L^1)(NO_3)_3]$ (II).** A solution of $Lu(NO_3)_3{\cdot}3H_2O$ (0.0466 g, 0.1123 mmol) in MeCN was added to a solution of ligand $L^1$ (0.0943 g, 0.1123 mmol) in MeCN. The yield was 0.113 g (84%), $T_m > 160$°C (decomp.).

For $C_{48}H_{42}N_{12}O_{13}PLu$

| | | | |
|---|---|---|---|
| Anal. calcd., % | C, 48.00 | H, 3.50 | N, 14.00 |
| Found, % | C, 48.04 | H, 3.65 | N, 14.02 |

**Study of extraction.** 1,2-Dichloroethane (reagent grade) was used as the organic solvent without additional purification. Solutions of extracting agent $L^2$ with a concentration of 0.05 mol/L were prepared using an exactly weighed sample. The initial aqueous solutions of U(VI), Th(IV), and Eu(III) were prepared by dissolution of the corresponding nitrates in water followed by the addition of $NH_4NO_3$. The initial concentration of the metal ions was $4 \times 10^{-6}$ mol/L, and that of $NH_4NO_3$ was 3 mol/L. The experiment was carried out according to the previously published procedure [20]. The distribution ratios of the elements ($D_M$) were calculated as the ratios of their concentrations in the equilibrium organic and aqueous phases ($D_M = [M_{org}]/[M_{aq}]$).

The quantum chemical calculations for the model complex $[La(L^3)(NO_3)_3]$ were performed using the ORCA, v. 4 software [22]. The relative energies of the complexes were calculated using the universal PBE0 functional [23] in the Def2-SVP basis set [24]. For the vibrational spectra interpretation, the normal virational modes (NCA) were calculated at the TPSS-D4/Def2-SVP level [25, 26]. The RIJCOSX approximation [27–29] with the auxiliary Def2/J basis set [30] was used to accelerate the calculations. Imaginary frequencies were absent for all calculated complexes.

The data on the quantum chemical calculations for the model complex $[La(L^3)(NO_3)_3]$ are given in the Supplementary Information (Scheme S2, Tables S1–S3, Fig. S22).

## RESULTS AND DISCUSSION

The hybrid tripodal ligands $L^1$ and $L^2$ can form coordination bonds with the lanthanide cations involving the phosphoryl group and/or nitrogen atoms of the triazole rings. The spectra indication of this coordination is the shift of the vibrational bands of the P=O bonds and triazole ring. The coordination of the P=O group of the ligands and nitrate ions is reliably determined from the IR spectral data [31]. The determination of the coordination of the triazole fragment is a more complicated spectral problem. In addition, the self-association of the ligands and developed intra- and intermolecular interactions involving the triazole fragments in the complexes [2, 32, 33] impede the interpretation of data of vibrational spectroscopy. Intermolecular interactions cleave on dissolution, which makes it possible to refine and check the deter-

**Table 1.** Frequencies of selected diagnostic bands in the IR spectra (ν, $cm^{-1}$) of solid compounds $L^1$ and $L^2$ and their complexes **I**–**III**, **V**, and **VI**

| Compound | ν(P=O) | $\nu(C_{tr}–H)$ | $\nu(NO_3)$ | Literature |
|---|---|---|---|---|
| $L^1$ | 1175 | 3130 br | | [14] |
| **I** | 1119 | 3137 br | ~1470, 1308 | This work |
| **II** | 1121 | 3137 br | 1502, 1307 | This work |
| **III** | 1175 | 3137 br | | [14] |
| $L^2$ | 1172 | 3149, 3130 sh | | [15] |
| **V** | 1117 | 3146 br | ~1470, 1308 | [15] |
| **VI** | 1127 | 3149 br | ~1520, 1300 | [15] |

mined assignments. An information about structures of compounds in solutions is of independent significance, since the practical application often requires the use of solutions, and the structures of compounds in the solid state and in solutions are not always identical.

In spite of the closely related structures, ligands $L^1$ and $L^2$ in crystals demonstrate different types of hydrogen bonds and short contacts involving the P(O) group and triazole rings. This is the bifurcated intramolecular hydrogen bond of the P(O) group with the C–H protons of two triazole rings in the crystal of $L^1$ [14], whereas in the crystal of $L^2$ these are hydrogen bonds via the water molecules with the triazole rings forming the dimer [15]. Complexes **I** and **II**, as well as complexes **V** and **VI**, were synthesized at a ligand to salt molar ratio of 1 : 1 and have the same composition. The selected band frequencies of solid complexes **I**, **II**, **V**, and **VI** compared to those for ligands $L^1$ and $L^2$ and palladium complex **III** are listed in Table 1.

In the IR spectra of solid ligands $L^1$ and $L^2$, the ν(P=O) frequency is somewhat lowered because of the formation of the corresponding hydrogen bonds [14, 15] observed at 1175 and 1172 $cm^{-1}$, respectively (Table 1). In the spectra of solid complexes **I**, **II**, **V**, and **VI**, the ν(P=O) band lies at 1119–1127 $cm^{-1}$, which indicates the coordination of the phosphoryl group with approximately the same strength (Table 1). The ν(P=O) frequency of the ligand remains unchanged in the spectrum of complex **III**, since the phosphoryl group does not participate in the coordination with Pd(II) and the complex is formed due to the coordination of two triazole rings of the ligand [14]. The nitrate anions in complexes **I**, **II**, **V**, and **VI** (Table 1) are coordinated in bidentate mode [31]. The expected low-intensity $\nu_s(NO_2)$ band at ~1030 $cm^{-1}$ is overlapped with the absorption of the triazole and phenyl rings.

The $\nu(C_{tr}–H)$ bands in the spectra of crystalline ligands $L^1$ and $L^2$ are consistent with the formation of the corresponding hydrogen bonds [14, 15]. The frequency of this vibration differs in the spectra of the solid complexes. In complexes **V** and **VI**, this vibrational frequency corresponds to the unbound $C_{tr}–H$ group [15]. In complexes **I**–**III**, the position of this band indicates weak intra- and intermolecular hydrogen contacts (Table 1).

The coordination of the triazole rings in the lanthanide complexes of ligand $L^2$ was determined according to the data of vibrational spectroscopy and quantum chemical calculations [15]. The vibration frequencies and modes were determined using normal coordinate analysis (NCA) for the model compounds [32] in which the triazole ring exhibits the same type of addition as that in ligand $L^2$. In both complexes **V** and **VI**, ligand $L^2$ exhibits the tetradentate $P(O),N^3,N^3,N^3$ coordination [15].

To determine the structures of the lanthanide complexes of ligand $L^1$, we performed the geometry optimization and calculated the normal vibrational modes at the TPSS-D4/Def2-SVP level for an isolated molecule of model complex **IV** containing triazole fragments of three types: uncoordinated, coordinated to the $N^2$ atom, and coordinated to the $N^3$ atom (Scheme 2), and three nitrate ions are coordinated in the bidentate mode. In complex **IV**, the coordination to the $N^3$ atom is stronger than that to the $N^2$ atom, which is indicated by a shorter (by ~0.1 Å) interatomic La...$N^3$ distance compared to the La...$N^2$ distance. Note that the higher strength of $N^3$ coordination compared to the coordination to the $N^2$ atom was described in many papers [1, 2, 5, 6, 12, 13].

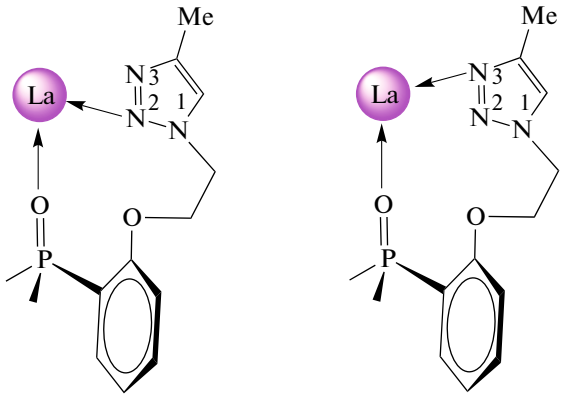


**Scheme 2.** Visualization of the $N^2$- and $N^3$-coordination modes of the triazole fragment in model complex **IV**.

A comparison of the Raman spectra of ligand $L^1$ and its complexes (Figs. 1, S5) shows that three Raman lines in the spectrum of the free ligand are sensitive to coordination: at 971 ($\nu_1$), 1042 ($\nu_2$), and 1358 ($\nu_3$) $cm^{-1}$. The lines of the ligand and complexes in the Raman spectra are somewhat broadened because of the developed intra- and intermolecular contacts of the triazole fragments. These additional interactions stabilizing the structures of the solid compounds are typical of 1,2,3-triazoles [2, 32]. In the IR spectra of the complexes, the corresponding changes are observed only for the $\nu_1$ band (Fig. S4). The band corresponding to the $\nu_2$ vibrational frequency is overlapped with the bands of the platform, and the $\nu_3$ band is very weak.

According to the NCA results, line $\nu_1$ refers to a mixed vibration with the predominant contribution of $\nu(N^1{-}N^2)$, line $\nu_2$ has the predominant contribution of the $C^5{-}C^4{-}N^3$ angle deformation, and line $\nu_3$ is assigned to vibrations of the $C^4{=}C^5$, $C^4{-}N^3$, and $C^5{-}N^1$ bonds. These frequencies change in different ways for different coordination modes (Table 2). The $\nu_1$ vibration frequency changes slightly (~2 $cm^{-1}$) upon the coordination to the $N^2$ atom, whereas it increases by ~30 $cm^{-1}$ on the coordination to the $N^3$ atom, which is likely associated with a change in the vibration shape. The $\nu_2$ vibration frequency decreases by ~10 $cm^{-1}$ when coordinating to the $N^2$ atom and decreases by ~10 $cm^{-1}$ for the coordination to the $N^3$ atom. The vibration frequency $\nu_3$ increases by ~5 $cm^{-1}$ upon the coordination to the $N^2$ atom and by ~10 $cm^{-1}$ for the coordination to the $N^3$ atom. The experimental vibration frequencies $\nu_1{-}\nu_3$ of ligand $L^1$ and their changes ($\Delta\nu$) upon coordination in complexes **I**–**III** and the calculated changes in the vibration frequencies of the free triazole fragment and this fragment coordinated in different coordination modes in model complex **IV** are compared in Table 2.

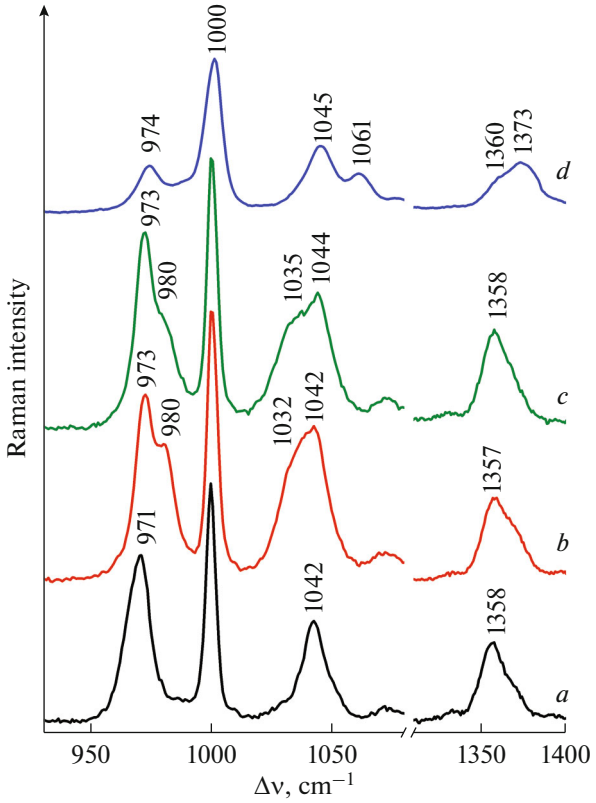


**Fig. 1.** Comparison of the fragments of the Raman spectra of solid compounds (a) $L^1$, (b) **I**, (c) **II**, and (d) **III**.

Palladium complex **III** has been described previously [14], but the N-coordination mode of the triazole rings was not refined.The IR spectrum of complex **III** (Fig. S4) shows the band at 1005 $cm^{-1}$ ($\Delta\nu$ = +34 $cm^{-1}$) along with the band at 971 $cm^{-1}$ ($\nu_1$). Upon coordination, the Raman line $\nu_1$ at 971 $cm^{-1}$ becomes less intense, and the maximum of the new line shifts, most likely, to the range of the intense broad line at ~1000 $cm^{-1}$ ($\Delta\nu$ = +29 $cm^{-1}$) (Fig. 1). A new line appears at 1061 $cm^{-1}$ ($\Delta\nu$ = +19 $cm^{-1}$) along with the Raman line $\nu_2$ at 1045 $cm^{-1}$, and the maximum of the $\nu_3$ line shifts to 1373 $cm^{-1}$ ($\Delta\nu$ = +15 $cm^{-1}$) (Fig. 2). These changes in the vibration spectra are consistent with the $N^3$ coordination of two triazole fragments, which seems most probable for the palladium complex. The coordination number of palladium in complex **III** is 4.

The Raman spectra of complexes **I** and **II** display a high-frequency shoulder at ~980 $cm^{-1}$ ($\Delta\nu$ = +9 $cm^{-1}$) along with the line at 973 $cm^{-1}$. The line at 1358 $cm^{-1}$ also has a high-frequency shoulder ($\Delta\nu$ = +7 $cm^{-1}$), and the $\nu_2$ line at ~1042 $cm^{-1}$ has a low-frequency shoulder ($\Delta\nu$ = −10 $cm^{-1}$) (Fig. 2). The IR spectrum of complex **I** exhibits band at 981 $cm^{-1}$ ($\Delta\nu$ = +10 $cm^{-1}$) along with the band at 971 $cm^{-1}$ ($\nu_1$).

**Table 2.** Experimental vibration frequencies of ligand $L^1$ and complexes **I**–**III** (ν, $cm^{-1}$), their shifts on coordination (Δν, $cm^{-1}$) in the Raman spectra, and calculated changes in the vibration frequencies for different coordination modes in model complex **IV** (calculation, Δν, $cm^{-1}$)

| Experiment, ν (Δν)[a] | | | | | Calculation for **IV**, Δν[b] | |
|---|---|---|---|---|---|---|
| ν | $L^1$ | **I** | **II** | **III** [14] | ($N^2$ coord.) | ($N^3$ coord.) |
| $\nu_1$ | 971 | 973, 980 (+9) | 973, ~980 sh (+9) | 974, 1000 (+29) | (+2) | (+30) |
| $\nu_2$ | 1042 | 1042, 1032 (−10) | 1044, 1035 (−7) | 1045, 1061 (+19) | (−10) | (+10) |
| $\nu_3$ | 1358 | 1357, ~1365 sh (+7) | 1358, ~1365 sh (+7) | 1360, 1373 (+15) | (+5) | (+10) |

[a] Δν = ν(complex) − ν($L^1$). [b] Δν = ν(coord.) − ν(free).

In the spectrum of complex **II**, this band is not resolved and has an "intermediate" maximum at 977 $cm^{-1}$ and a high-frequency shoulder (Fig. S4).

The set of quantum chemical calculations and vibration spectra of lanthanide complexes **I** and **II** suggests that the ligand molecule is coordinated in the P(O),$N^2$,$N^2$-tridentate mode and three nitrate ions are coordinated in the bidentate mode in both complexes [Ln{P(*O*),$N^2$,$N^2$-$L^1$}(O,O-$NO_3$)$_3$] (Ln = La, Lu) (Scheme 3). For both lanthanides, the coordination number is 9, which is typical of the majority of complexes of these metals.

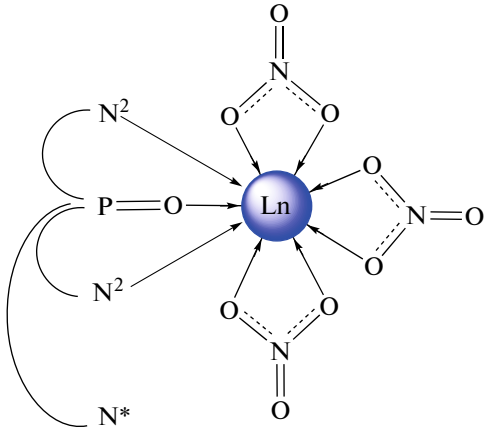


**Scheme 3.** Structure of the [Ln{P(*O*),$N^2$,$N^2$-$L^1$}(O,O-$NO_3$)$_3$] complexes (Ln = La, Lu) in the solid state and in solutions. Symbol N* designates the "free" (uncoordinated) triazole cycle involved in additional intra- and intermolecular contacts.

It is noteworthy that the "free" triazole fragments of both the ligands and complexes are almost always involved in the system of weak intra- and intermolecular interactions and hydrogen bonds [2, 32, 33]. Therefore, the lines in the Raman spectra of individual compounds are somewhat broadened, and the IR spectra are more complicated. New couplings appear instead of these interactions in solutions and, hence, the structures of the compounds in the solution and in the solid phase can differ substantially.

The structures of the complexes in solutions were studied by IR and multinuclear NMR spectroscopy. The solvents with different acid–base properties and different dielectric constants (ε) were used: $CDCl_3$ (ε = 4) and $CD_3CN$ (ε = 36).

The structures of free ligands $L^1$ and $L^2$ in solutions differ. The intramolecular hydrogen bond found in the crystal of $L^1$ is retained in solutions [14]. The ν(P=O) band corresponds to the bound phosphoryl group like in the spectrum of the crystalline sample. The ν($C_{tr}$–H) band has maxima at 3144 and 3115 $cm^{-1}$ belonging to the free and H-bound triazole rings. The intermolecular hydrogen bonds found in the crystal of $L^2$ are cleaved upon dissolution, and the spectra correspond to that of individual molecule [15]. The ν(P=O) vibration frequency is 1186 and 1174 $cm^{-1}$ in acetonitrile and chloroform solutions, respectively (decreasing frequency in $CDCl_3$ is caused by solvation). The ν($C_{tr}$–H) frequency at 3143 (in $CD_3CN$) and 3148 $cm^{-1}$ (in $CDCl_3$) corresponds to the free triazole cycles.

The structures of complexes **V** and **VI** in solutions were determined by the data of IR spectroscopy, NMR spectroscopy, and quantum-chemical calculations [15]. In acetonitrile solutions, both complexes are ionic and represent contact ion pairs with the tetradentate-coordinated ligand [Ln{P(*O*),$N^3$,$N^3$,$N^3$-$L^2$}(O,O-$NO_3$)$_2$]$^+$·($NO_3$)$^-$ (Ln = La, Lu), and the lanthanum complex [La{P(*O*),$N^3$,$N^3$,$N^3$-$L^2$}(O,O-$NO_3$)$_3$]$^0$ is neutral in chloroform.

Selected spectral data for solutions of ligands $L^1$ and $L^2$ and their lanthanide complexes **I**, **II**, **V**, and **VI** are given in Tables 3 and 4. Since the interpretation of the IR spectra of the solutions was impeded by band superpositions, we used the decomposition of the bands and the difference spectra to refine the changes (Figs. S7, S9).

As in the case of the solid compounds, the coordination of the phosphoryl group and bidentate coordination of the nitrate ions are reliably determined from the IR spectra. The spectral manifestations of these interactions are nearly the same for the lanthanide complexes of both ligands (Tables 3, 4). Minor distinctions (split band of the phosphoryl group) were observed for a solution of complex **II** in $CD_3CN$

**Table 3.** Selected data of the IR (ν, $cm^{-1}$) and $^{31}P\{^1H\}$, $^{13}C$ NMR (δ, ppm) spectra of ligand $L^1$ and complexes **I** and **II** in $CD_3CN$ and $CDCl_3$ (0.01 mol/L) at 298 K

| Compound | Solvent | ν(P=O) | Vibrations of triazole cycle | $\delta_P(W_{1/2})$[a] | $\delta_C(C^4)$ | $\delta_C(\underline{C}^5–H)$ |
|---|---|---|---|---|---|---|
| $L^1$ | $CD_3CN$[b] | 1176 | 973[c] | 24.5 s (0.02) | 146.91 s | 122.43 s |
| | $CDCl_3$[b] | 1174 [20] | | 25.2 s (0.2) | 147.51 s | 122.09 s |
| **I** | $CD_3CN$ | 1124 | 973, 983 | 31.8 s (0.6) | 146.62 s | 121.95 s |
| | $CDCl_3$ | 1119 | 974 | 38.9 s (0.5), 31.8 s (1.3)[d] | 147.2 br.s | 121.2 vbr.s |
| **II** | $CD_3CN$ | 1128, 1118 | 973 | 35.3 s (1.0) | 146.73 s | 121.26 s |
| | $CDCl_3$ | 1116 | 974 | 45.2 s (0.5), 37.6 s (1.4)[d] | 147.3 br.s<br>147.5 br.s | 121.4 br.s |

[a] Signal half-width at half-height (ppm).
[b] Intramolecular hydrogen bond in molecule $L^1$ (see text).
[c] Absorption of the solvent does not allow the determination of the position of the weak maximum.
[d] Ratio of integral intensities ~1 : 1.

**Table 4.** Selected data of the IR (ν, $cm^{-1}$) and $^{31}P\{^1H\}$, $^{13}C$ NMR (δ, ppm) spectra of ligand $L^2$ and complexes **V** and **VI** in $CD_3CN$ and $CDCl_3$ (0.01 mol/L) at 298 K [15]

| Compound [15] | Solvent | ν(P=O), $cm^{-1}$ | Vibrations[a] of triazole cycle, $cm^{-1}$ | $\delta_P(W_{1/2})$[b] | δ($C^4$) | δ($\underline{C}^5$–H) |
|---|---|---|---|---|---|---|
| $L^2$ | $CD_3CN$ | 1186 | 1046[a], 1037 | 22.0 s (0.16) | 144.21 s | 121.74 s |
| | $CDCl_3$ | 1174 | 1044[a], 1037 | 26.0 s (0.3) | 144.39 s | 121.43 s |
| **V** | $CD_3CN$ | 1119 | 1066[c] | 31.4 s (0.2) | 143.24 s | 121.81 s |
| | $CDCl_3$ | 1119 | 1066[c] | 30.9 s (1.3) | 143.5 3s | 121.47 s |
| **VI**[d] | $CD_3CN$ | 1128 | 1070 br[c] | 34.1 s (0.18) | 143.18 s | 122.03 s |

[a] Deformation band of triazole rings is overlapped with the band of platform vibrations.
[b] Signal half-width at half-height (ppm).
[c] Data of the difference spectra.
[d] Complex insoluble in chloroform.

(Table 3). In the first approximation, the bands of the nitrate groups correspond to their bidentate coordination [31]: ~1470, ~1310, and shoulders at ~1300, 1030 $cm^{-1}$ for solutions of the lanthanum complexes; and ~1510, ~1310, and 1030 $cm^{-1}$ for the lutetium complexes. However, the bands are somewhat complicated, which is determined, as known, by the type of species (neutral complex, contact ion pair, ion pair separated by solvent, etc.) and also by the symmetric or nonsymmetric environment of the ion in these species. Additional weak bands at ~1398 and ~1356 $cm^{-1}$ are observed in the IR spectra of the complexes of $L^1$ in $CDCl_3$ solutions.

The coordination of the triazole fragments in solutions of the complexes of $L^2$ was determined by the shift of the deformation band of the triazole cycle at ~1040 $cm^{-1}$ toward high frequencies [15]. Only one shifted band at ~1070 $cm^{-1}$ is observed in the difference spectra of solutions of complexes **V** and **VI** (Table 4).

Two indicators were used to attribute coordination mode of the triazole rings for the complexes of ligand $L^1$. According to the calculation for $N^3$ coordination, the weak band at 971 $cm^{-1}$ corresponding to the $\nu_1$ vibrations should shift by +30 $cm^{-1}$. The medium-intensity IR bands in a range of ~1040–1070 $cm^{-1}$, where the deformation bands of the triazole rings and planar δ(CH) vibrations of the benzene rings of the platform are overlapped, undergo shifts by +2 $cm^{-1}$ upon the $N^2$ coordination. According to the calculation, the latter are sensitive to the conformation of the whole triazole branch, which changes upon both coordination and intramolecular interactions involving the triazole fragment, rather than to the coordination of triazoles. Therefore, the IR spectra of the complexes and ligand $L^1$ in a range of 1040–

1070 $cm^{-1}$ differ (Figs. S6–S9), which makes it possible to preliminarily conclude about the involvement of the triazole rings in coordination, but without revealing details of the coordination mode.

In the IR spectra of solutions of complexes **I** and **II** and in the spectra of the solid complexes, the band at 973 $cm^{-1}$ ($\nu^1$) retains its position and becomes more intense. A weak band at 983 $cm^{-1}$ appears additionally in the spectrum of a solution of complex **I** in $CD_3CN$. This position of the $\nu_1$ band is consistent with the coordination of the triazole fragments to the $N^2$ atom (Figs. S6–S9). Two bands are observed in the range of ~1040–1070 $cm^{-1}$ in the spectra of solutions of complexes **I** and **II**: the more intense mixed band at ~1070 and the band at ~1050 $cm^{-1}$ close in frequency to the band of the ligand (Figs. S6–S9). It can be assumed that in solutions ligand $L^1$ also exhibits the P(O),$N^2$,$N^2$ coordination with the lanthanide cations, and the third "free" triazole branch also experiences a change in the conformation being involved in additional intramolecular interactions (similarly to the intramolecular hydrogen bonds of the ligand itself in solutions).

Higher spectral differences were found when comparing the NMR spectra of solutions of the complexes of two ligands $L^1$ and $L^2$.

One signal shifted relative to the signal of the free ligand [15] is observed in the $^{31}P$ NMR spectra of complexes **V** and **VI** in both solvents (Table 4). For complexes **I** and **II**, one shifted singlet is observed only in the spectra of solutions in $CD_3CN$ (which is significantly broadened in the spectrum of complex **II**), whereas two shifted signals of different widths and approximately the same integral intensity are detected in the spectra of $CDCl_3$ solutions (Table 3, Figs. S12, S15, S18, S21).

In the $^1H$ NMR spectra, narrow signals are observed only for acetonitrile solutions of the lanthanum complexes of both ligands (**I** and **V**). In both cases, the signals in the spectra are broadened or significantly broadened, which indicates dynamic equilibria involving the complexes with different structures (Tables 3, 4; Figs. S10, S13, S16, S19).

The signals in the $^{13}C$ NMR spectra of all solutions of the complexes of $L^2$ are narrow, whereas for the complexes of $L^1$ one set of narrow signals is observed only for solutions in $CD_3CN$, and the signals of the indicatory nuclear of complexes **I** and **II** are broadened and doubled in the spectra of $CDCl_3$ solutions (Tables 3, 4; Figs. S11, S14, S17, S20). The shifts occurred upon coordination for the signals of the indicatory nucleus of the triazole rings $C^4_{tr}$ of complexes **V** and **VI** are nearly 1 ppm, whereas they do not exceed 0.2–0.3 ppm for complexes **I** and **II** (Tables 3, 4). This indicates weaker coordination interactions of the triazole fragments in the complexes of $L^1$, which are close in strength to the additional intramolecular contacts involving these groups.

The positions of the $C^5_{tr}$–H signals in the spectra of solutions of complexes **V** and **VI** are nearly identical to the signals of the free ligand (Table 4), whereas they are substantially shifted in the spectra of complexes **I** and **II** (Table 3). This distinction can be assumed as caused by the difference in both the coordination mode of the ligands and involvement of the $C_{tr}{}^5$–H groups of the uncoordinated triazole rings of the ligand $L^1$ in additional intramolecular interactions (e.g., [32]).

The set of the IR and NMR spectral data (Table 3) and results of quantum chemical calculation suggest that an acetonitrile solution of complex **I** contains one mononuclear neutral complex [La{P(*O*),$N^2$,$N^2$-$L^1$}(O,O-$NO_3$)$_3$]$^0$ in which two triazole fragments are coordinated to the $N^2$ atom of the ring and the third fragment is involved in the intramolecular interactions (Scheme 3). The main component of complex **II** in a $CD_3CN$ solution has the same structure, but the solution also contains two (or several) species of similar structure differed in specific features of the coordination of the P=O group group (broadened signals in $^{31}P$ and $^1H$ NMR spectra, split ν(P=O) band in the IR spectrum). For example, the isomer with the $C_{tr}$-H...O=P intramolecular interaction (similar to the intramolecular hydrogen bond in free ligand $L^1$) or the isomer with the O,$N^2$-coordinated ligand.

Complexes **I** and **II** experience substantial changes in chloroform. The emergence of two signals in the $^{31}P$ NMR spectra suggests [34–36] the presence of neutral complex [Ln{P(*O*),$N^2$,$N^2$-L1}(O,O-$NO_3$)$_3$]$^0$ (coordination number 9) and ionic complex (in the form of a contact ion pair) [Ln{P(*O*),$N^2$,$N^2$-$L^1$}(O,O-$NO_3$)$_2$]$^+$ $(NO_3)^-$ (coordination number 7) (Ln = La, Lu) in equilibrium. The complication of the band of the nitrate ions and the emergence of additional low-intensity bands at 1356 and 1397 $cm^{-1}$ in the IR spectra are consistent with this assumption. The broadening of one of the signals in the $^{31}P$ NMR spectra can also be caused by the presence of additional minor species, for example, [Ln{P(*O*),$N^2$-$L^1$}(O,O-$NO_3$)$_3$]$^0$ (Ln = La, Lu), in equilibrium.

In $^1H$ NMR spectra of complexes **I** and **II** in chloroform, all signals are significantly broadened and the $CH_2$ signals of the linker are doubled and broadened. In the $^{13}C$ NMR spectrum, only the signals of the phenyl substituent in the triazole cycle and the signal of the $CH_2N$ linker are narrow, and all other signals are broadened and doubled, which agrees with two signals in the $^{31}P$ NMR spectrum and suggests the presence of two main ~1 : 1 neutral and ionic complexes in equilibrium in the solution.

The large signal broadening and complication of spectra of lutetium complex **II** compared to the spectra of lanthanum complex **I** suggest that the solution of complex **II** contains larger amount of minor species, for example, neutral complex $[Lu\{P(O)\text{-}L^1\}(O,O\text{-}NO_3)_3(H_2O)_n]^0$ (coordination number 7 or 8) with the "free" triazole rings solvated by chloroform (in the $^{13}C$ NMR spectrum, the signal corresponding to that of the free ligand in $CDCl_3$ is observed along with the broadened $\delta_C(C^4_{tr})$ signal shifted by 0.2 ppm only) (Table 3).

Thus, ligands $L^1$ and $L^2$ differed by the type of addition of the 1,2,3-triazole fragment and linker length exhibit different coordination properties in the complexes with lanthanide nitrates, and the main difference is the change in the N-coordination mode of the triazole fragment and denticity of the ligand. The tridentate $P(O),N^2,N^2$ coordination is observed for the complexes of $L^1$ instead of the tetradentate $P(O),N^3,N^3,N^3$ coordination found for the complexes of $L^2$ [15]. This distinction found for the solid complexes is retained in solutions ($CD_3CN$, $CDCl_3$).

One more important factor is a change in the type of complexes when replacing the solvent. For instance, in $CD_3CN$ the complexes of ligand $L^2$ are ionic and the complexes of $L^1$ are neutral. An equilibrium of the neutral and ionic complexes of $L^1$ in ~1 : 1 ratio is observed in $CDCl_3$, whereas the complexes of $L^2$ are neutral.

The extraction properties of closely related compounds $L^1$ and $L^2$ toward the *f* elements were studied for the extraction of microquantities of U(VI), Th(IV), and Eu(III) from aqueous solutions to 1,2-dichloroethane (DCE). Ligand $L^2$ turned out to extract U(VI), Th(IV), and Eu(III) from neutral aqueous solutions to DCE ~70–10 times more efficiently than ligand $L^1$ does (Table 5).

The efficiency of extraction is known to be determined by many factors, including the compositions, strengths, and structures of the extracted complexes, as well as the lipophilicity of the extracting agent and its complexes. The structures of the extracted complexes can differ from those of individual (model) compounds. However, the data on the structures of the latter in solutions can successfully be used in an analysis of the extraction properties of the related compounds. A qualitative correlation between the efficiency and structure (strength) of the model complexes was observed by many researchers for related extracting agents [32, 37–41].

The lipophilicities of related ligands $L^1$ and $L^2$ are evidently close, and the entropy component of the complexation accompanied by the formation of large nine- and ten(eleven)-membered chelate rings should be close. Therefore, it can be expected that different coordination properties of compounds $L^1$ and $L^2$ are the main factors that cause their different extraction properties. The data on the structures of the ligands and lanthanide complexes in nonpolar chloroform were used to compare extraction efficiency.

**Table 5.** Extraction properties of ligands $L^1$ and $L^2$*

| Compound | Distribution ratios** | | |
|---|---|---|---|
| | $D_U$ | $D_{Th}$ | $D_{Eu}$ |
| $L^1$ [20] | 2.9 | 0.49 | 0.0007 |
| $L^2$ | 200 | 2.2 | 0.004 |

* Results of the studies of the uranyl complexes will be published elsewhere. ** $D_M = [M]_{org}/[M]_{aq}$, where M is metal.

The structures of the model complexes of ligands $L^1$ and $L^2$ in chloroform differ substantially. The lanthanum complex of ligand $L^2$ (**V**) in chloroform is neutral, ligand $L^2$ is coordinated in the $P(O),N^3,N^3,N^3$-tetradentate mode, and the triazole fragments are coordinated more strongly than those in the complexes of ligand $L^1$. Unlike this complex, the lanthanum complex of ligand $L^1$ (**I**) in chloroform represents a ~1 : 1 equilibrium mixture of neutral and ionic species, like complex **II**. The strength of the coordination of the P(O) group in the complexes of $L^1$ is almost the same as in the complexes of $L^2$, and the coordination of the triazole fragments is weaker. It can be expected that the complexes of europium (as lanthanide of the middle of the row) will be similar in structure. Since the neutral complexes are more lipophilic and are extracted to an organic solvent to a higher extent than the ionic complexes, the efficiency of extraction of lanthanides (in particular, Eu) by extracting agent $L^2$ will be higher than that by $L^1$ (Table 5). In addition, unlike ligand $L^2$, the intramolecular hydrogen bond in solutions of ligand $L^1$ is retained. Therefore, a less strong coordination of the triazole fragments (lower strength of the complexes), the presence of a significant fraction of the ionic complexes, and retention of the intramolecular hydrogen bond in ligand $L^1$ itself in solutions are likely reasons for a lower efficiency of lanthanide extraction by ligand $L^1$ compared to $L^2$.

Thus, the coordination and extraction properties of two related tripodal ligands on the $Ph_3P(O)$ platform with the 1,2,3-triazole rings in the pendants, which differ in the type of addition of the triazole fragment and the linker length in compounds $L^1$ and $L^2$, were studied and compared.

The compositions and structures of the $[Ln(NO_3)_3L^1]$ complexes (where Ln = $La^{3+}$, $Lu^{3+}$) were studied in the solid state (elemental analysis, IR and Raman spectroscopy) and in $CD_3CN$ and $CDCl_3$ solutions (IR and multinuclear $^1H$, $^{13}C$, and $^{31}P$ NMR spectroscopy). For the correct interpretation of the vibrational spectra of the complexes of ligand $L^1$, we

performed geometry optimization and calculated the frequencies and modes of the normal vibrations at the TPSS-D4/Def2-SVP level for an isolated molecule of the model complex [La{P(*O*),$N^3$,$N^2$-$L^3$}(O,O-$NO_3$)$_3$] (**IV**), which contains three types of triazole fragments: uncoordinated, coordinated to the $N^2$ atom, and coordinated to the $N^3$ atom; and three nitrate ions are coordinated in the bidentate mode. Ligand $L^3$ with the Me substituents in the triazole ring was used as a simpler model in the quantum chemical calculations instead of ligand $L^1$. According to the set of spectral and quantum chemical data, ligand $L^1$ exhibits the tridentate P(O),$N^2$,$N^2$ coordination in the lanthanide complexes. These are neutral complexes in the solid state and in $CD_3CN$ solutions, and the dynamic equilibrium of the neutral and ionic complexes is observed in $CDCl_3$.

Unlike ligand $L^1$, ligand $L^2$ exhibits the tetradentate P(O),$N^3$,$N^3$,$N^3$ coordination in the complexes with the same metals [15]. These are ionic complexes (contact ion pairs) in the solid phase and in $CD_3CN$ solutions, and they are neutral in $CDCl_3$ solutions [15].

According to the spectral data, the strength of the P(O) coordination in the complexes of both ligands is similar, but the strengths of the $N^2$- and $N^3$-coordination modes of the triazole fragments differ. A change in the coordination mode of the ligand, the type of the complexes (ionic, neutral), and the presence or absence of an intramolecular hydrogen bond in the ligand molecule in solutions make it possible to explain differences in the efficiency of lanthanide extraction by the related ligands $L^1$ and $L^2$.

Thus, the change in the type of addition of the 1,2,3-triazole ring (C- or N-addition) drastically changes the extraction and coordination properties of the studied compounds.

The obtained results demonstrate that the use of the C-addition of 1,2,3-triazole rings is promising for the synthesis of tripodal ligands as efficient complexing and extracting agents for the recovery of *f* elements.

## SUPPLEMENTARY INFORMATION

The online version contains supplementary material available at https://doi.org/10.1134/S1070328423601000.

## ACKNOWLEDGMENTS

Elemental analysis and NMR, IR, and Raman spectra recording were supported by the Ministry of Science and Higher Education of the Russian Federation using the scientific equipment of the Nesmeyanov Institute of Organoelement Compounds (Russian Academy of Sciences).

## FUNDING

This work was supported by the Russian Science Foundation, project no. 20-13-00329.

## CONFLICT OF INTEREST

The authors of this work declare that they have no conflicts of interest.

## REFERENCES

1. Aromí, G., Barrios, L.A., Roubeau, O., et al., *Coord. Chem. Rev.*, 2011, vol. 255, p. 485.
2. Schulze, B. and Schubert, U.S., *Chem. Soc. Rev.*, 2014, vol. 43, p. 2522.
3. Götzke, L., Schaper, G., März, J., et al., *Coord. Chem. Rev.*, 2019, vol. 386, p. 267.
4. Scattergood, P., Sinopoli, A., and Elliott, P., *Coord. Chem. Rev.*, 2017, vol. 350, p. 136.
5. Huang, D., Zhao, P., and Astruc, D., *Coord. Chem. Rev.*, 2014, vol. 272, p. 145.
6. Hosseinnejad, T., Ebrahimpour-Malmir, F., and Fattahi, B., *RSC Adv.*, 2018, vol. 22, no. 8, p. 12232.
7. Lauko, J., Kouwer, P.H.J., and Rowan, A.E., *J. Heterocycl. Chem.*, 2017, vol. 54, no. 3, p. 1677.
8. Nößler, M., Hunger, D., Neuman, N.I., et al., *Dalton Trans.*, 2022, vol. 51, p. 10507.
9. Urankar, D., Pinter, B., Pevec, A., et al., *Inorg. Chem.*, 2010, vol. 49, p. 4820.
10. Guha, P.M., Phan, H., Kinyon, J.S., et al., *Inorg. Chem.*, 2012, vol. 51, p. 3465.
11. Kilpin, K.J., Gavey, E.L., McAdam, C.J., et al., *Inorg. Chem.*, 2011, vol. 50, p. 6334.
12. Lo, W.K.C., Huff, G.S., Cubanski, J.R., et al., *Inorg. Chem.*, 2015, vol. 54, no. 4, p. 1572.
13. Saleem, F., Rao, G.K., Kumar, A., et al., *Organometallics*, 2013, vol. 32, no. 13, p. 3595.
14. Kudryavtsev, I.Y., Bykhovskaya, O.V., Matveeva, A.G., et al., *Monats. Chem.*, 2020, vol. 151, no. 11, p. 1705.
15. Matveeva, A.G., Bykhovskaya, O.V., Pasechnik, M.P., et al., *Mendeleev Commun.*, 2022, vol. 32, no. 5, p. 588.
16. Platt, A.W.G., *Coord. Chem. Rev.*, 2017, vol. 340, p. 62.
17. Bryleva, Yu.A., Artem'ev, A.V., Glinskaya, L.A., et al., *J. Struct. Chem.*, 2021, vol. 62, no. 2, p. 265. https://doi.org/10.1134/S0022476621020116
18. Bryleva, Yu.A., Artem'ev, A.V., Glinskaya, L.A., et al., *New J. Chem.*, 2021, vol. 45, p. 13869.
19. Bryleva, Y.A., Komarov, V.Yu., Glinskaya, L.A., et al., *New J. Chem.*, 2023, vol. 47, p. 10446.
20. Matveeva, A.G., Baulina, T.V., Kudryavtsev, I.Yu., et al., *Russ. J. Gen. Chem.*, 2020, vol. 90, no. 12, p. 2338. https://doi.org/10.1134/S107036322012018X
21. Armarego, W.L.F. and Chai, C.L.L., *Purification of Laboratory Chemicals*, New York: Elsevier, 2009.
22. Neese, F., *WIREs Comput. Mol. Sci.*, 2018, vol. 8, no. 1, p. e1327.
23. Adamo, C. and Barone, V., *J. Chem. Phys.*, 1999, vol. 110, no. 13, p. 6158.

24. Weigend, F. and Ahlrichs, R., *Phys. Chem. Chem. Phys.*, 2005, vol. 7, no. 18, p. 3297.
25. Perdew, J.P., Ruzsinsky, A., Csonka, G.I., et al., *Phys. Rev. Lett.*, 2009, vol. 103, p. 026403.
26. Caldeweyher, E., Bannwarth, C., and Grimme, S., *J. Chem. Phys.*, 2017, vol. 147, p. 034112.
27. Neese, F., *J. Comput. Chem.*, 2003, vol. 24, no. 14, p. 1740.
28. Neese, F., Wennmohs, F., Hansen, A., et al., *Chem. Phys.*, 2009, vol. 356, nos. 1–3, p. 98.
29. Dutta, A.K., Neese, F., and Izsak, R., *J. Chem. Phys.*, 2016, vol. 144, no. 3, p. 034102.
30. Weigend, F., *Phys. Chem. Chem. Phys.*, 2006, vol. 8, no. 9, p. 1057.
31. Nakamoto, K., *Infrared and Raman Spectra of Inorganic and Coordination Compounds*, Hoboken: Wiley, 2009.
32. Matveeva, A.G., Vologzhanina, A.V., Pasechnik, M.P., et al., *Polyhedron*, 2022, vol. 215, p. 115680.
33. Mohammadsaleh, F., Jahromi, M.D., Hajipour, A.R., et al., *RSC Adv.*, 2021, vol. 11, no. 34, p. 20812.
34. Matveeva, A.G., Peregudov, A.S., Matrosov, E.I., et al., *Inorg. Chim. Acta*, 2009, vol. 362, p. 3607.
35. Davis, M.F., Levason, W., Ratnani, R., et al., *New J. Chem.*, 2006, vol. 30, p. 782.
36. Matveeva, A.G., Kudryavtsev, I.Yu., Pasechnik, M.P., et al., *Polyhedron*, 2018, vol. 142, p. 71.
37. Kiefer, C., Wagner, A.T., Beele, B.B., et al., *Inorg. Chem.*, 2015, vol. 54, p. 7301.
38. Matveeva, A.G., Vologzhanina, A.V., Goryunov, E.I., et al., *Dalton Trans.*, 2016, vol. 45, p. 5162.
39. Bremer, A., Ruff, C.M., Girnt, D., et al., *Inorg. Chem.*, 2012, vol. 51, p. 5199.
40. Matveeva, A.G., Artyushin, O.I., Pasechnik, M.P., et al., *Polyhedron*, 2021, vol. 198, p. 115085.
41. Beele, B.B., Rüdiger, E., Schwörer, F., et al., *Dalton Trans.*, 2013, vol. 42, p. 12139.

*Translated by E. Yablonskaya*